

# Project 3: Wiener-Bose Model

Eric LaForest

April 9, 2010

## Contents

<b>1</b>	<b>Model</b>	<b>3</b>
<b>2</b>	<b>Analysis Method</b>	<b>4</b>
2.1	Laguerre Functions . . . . .	4
2.2	Finding and Refining $\alpha$ . . . . .	4
2.2.1	Most Significant Kernel . . . . .	4
<b>3</b>	<b>Results</b>	<b>5</b>
3.1	FHN System Response . . . . .	5
3.2	Determining $L$ . . . . .	6
3.2.1	Determining $L$ via Memory-Bandwidth Product . . . . .	6
3.2.2	Determining $L$ via Laguerre Coefficients . . . . .	7
3.3	First and Second-Order Kernels . . . . .	8
3.4	Wiener-Bose Model under GWN Stimuli . . . . .	9
3.4.1	Low-Power Mode . . . . .	9
3.4.2	High-Power Mode . . . . .	11
3.5	Wiener-Bose Model under Other Stimuli . . . . .	13
3.5.1	Low-Power Mode under Constant Stimulus . . . . .	13
3.5.2	Low-Power Mode under Periodic Stimulus . . . . .	14
3.5.3	High-Power Mode under Constant Stimulus . . . . .	15
3.5.4	High-Power Mode under Periodic Stimulus . . . . .	16

## List of Tables

1	Mean Square Error of Low-Power WB Model Response Relative to FHN System Response . . . . .	9
2	Mean Square Error of High-Power WB Model Response Relative to FHN System Response . . . . .	11

## List of Figures

1	Subthreshold FHN System under GWN1 Stimulus . . . . .	5
2	Suprathreshold FHN System under GWN1 Stimulus . . . . .	5
3	Frequency Spectrum of Subthreshold FHN System Response . . . . .	6
4	Frequency Spectrum of Suprathreshold FHN System Response . . . . .	6
5	First-Order Lee-Schetzen Kernel of Low-Power Wiener-Bose Model . . . . .	6
6	First-Order Lee-Schetzen Kernel of High-Power Wiener-Bose Model . . . . .	6
7	Coefficients of First-Order Kernel of Low-Power Wiener-Bose Model . . . . .	7
8	Coefficients of First-Order Kernel of High-Power Wiener-Bose Model . . . . .	7
9	First-Order Kernel of Low-Power Wiener-Bose Model ( $\alpha = 0.95$ ) . . . . .	8
10	Second-Order Kernel of Low-Power Wiener-Bose Model ( $\alpha = 0.95$ ) . . . . .	8
11	First-Order Kernel of High-Power Wiener-Bose Model ( $\alpha = 0.94$ ) . . . . .	8
12	Second-Order Kernel of High-Power Wiener-Bose Model ( $\alpha = 0.94$ ) . . . . .	8
13	Comparison of Low-Power Wiener-Bose Model to FHN System (GWN1) . . . . .	9
14	Comparison of Low-Power Wiener-Bose Model to Subthreshold FHN System(GWN2) . . . . .	10
15	Comparison of Low-Power Wiener-Bose Model to Subthreshold FHN System (GWN3) . . . . .	10
16	Comparison of High-Power Wiener-Bose Model to Suprathreshold FHN System (GWN1) . . . . .	11
17	Comparison of High-Power Wiener-Bose Model to Suprathreshold FHN System (GWN2) . . . . .	12
18	Comparison of High-Power Wiener-Bose Model to Suprathreshold FHN System (GWN3) . . . . .	12
19	Low-Power Wiener-Bose Model of FHN System (Constant Zero Stimulus) . . . . .	13
20	Low-Power Wiener-Bose Model of FHN System (Constant 1 Stimulus) . . . . .	13
21	Low-Power Wiener-Bose Model of FHN System (Constant 1.455 Stimulus) . . . . .	13
22	Low-Power Wiener-Bose Model of FHN System (Constant -1 Stimulus) . . . . .	13
23	Low-Power Wiener-Bose Model of FHN System (Constant 0.33 Stimulus) . . . . .	13
24	Low-Power Wiener-Bose Model of FHN System ( $\cos(t)$ Stimulus) . . . . .	14
25	Low-Power Wiener-Bose Model of FHN System ( $1.455\cos(t)$ Stimulus) . . . . .	14
26	Low-Power Wiener-Bose Model of FHN System ( $1.455\cos(0.33t)$ Stimulus) . . . . .	14
27	Low-Power Wiener-Bose Model of FHN System ( $0.33\cos(t)$ Stimulus) . . . . .	14
28	Low-Power Wiener-Bose Model of FHN System ( $0.33\cos(0.33t)$ Stimulus) . . . . .	14
29	High-Power Wiener-Bose Model of FHN System (Constant 0 Stimulus) . . . . .	15
30	High-Power Wiener-Bose Model of FHN System (Constant 1 Stimulus) . . . . .	15
31	High-Power Wiener-Bose Model of FHN System (Constant 1.455 Stimulus) . . . . .	15
32	High-Power Wiener-Bose Model of FHN System (Constant -1 Stimulus) . . . . .	15
33	High-Power Wiener-Bose Model of FHN System (Constant 0.33 Stimulus) . . . . .	15
34	High-Power Wiener-Bose Model of FHN System ( $\cos(t)$ Stimulus) . . . . .	16
35	High-Power Wiener-Bose Model of FHN System ( $1.455\cos(t)$ Stimulus) . . . . .	16
36	High-Power Wiener-Bose Model of FHN System ( $1.455\cos(0.33t)$ Stimulus) . . . . .	16
37	High-Power Wiener-Bose Model of FHN System ( $0.33\cos(t)$ Stimulus) . . . . .	16
38	High-Power Wiener-Bose Model of FHN System ( $0.33\cos(0.33t)$ Stimulus) . . . . .	16

# 1 Model

The system for this simulation is the FitzHugh-Nagumo (FHN) model:

$$\dot{V} = V - \frac{V^3}{3} - W + F(t)$$

$$\dot{W} = 0.08(V + 0.7 - 0.8W)$$

with initial conditions  $V = -1.1994$  and  $W = -0.6243$ , which is the resting state of this system after a finite perturbation followed by a sufficiently long constant zero input.

The FHN system is driven by a zero-mean, filtered, Gaussian White Noise (GWN) stimulus  $F(t)$ . Two versions of the GWN are used: a low-power GWN which does not cause action potentials, and a high-power GWN which does. Experimentation showed that a peak value of  $\pm 2$  yields low-power behaviour, while peaks of  $\pm 10$  yields high power behaviour. The effective frequency of this GWN was set to 10Hz by specifying 20 points to be generated over the time interval of 0 to 1, as per the Nyquist criterion<sup>1</sup>. Repeating this 10 times yields 2000 points over 100 seconds. One set (GWN1) is used for fitting, and two others (GWN2, GWN3) are used for testing.

The following experiments attempt to map the FHN system to a second-order Wiener-Bose (WB) model. The WB parameters are the number of Laguerre functions ( $L$ ), the scaling of their convolutions ( $\alpha$ ), and the number of points in each kernel (which is always taken to be 512, the maximum allowed). The GWN stimulus generation and the WB analyses are mostly done using the LYSIS tools, while the FHN responses and frequency spectra were calculated in MATLAB 7.8.

---

<sup>1</sup>2 samples per cycle minimum, therefore 20 samples equal 10 cycles

## 2 Analysis Method

The overall scheme to fit the WB model to the responses of the FHN system is as follows:

1. Determine the number of Laguerre functions required
2. Find a suitable  $\alpha$  factor such that the most significant kernel fits inside its 512 points
3. Refine this estimate of  $\alpha$  to minimize the Mean Square Error (MSE) between the FHN system response and the WB model response.

### 2.1 Laguerre Functions

The number of Laguerre functions ( $L$ ) required to build an effective WB model can be determined in several ways:

- The product of the system memory and its bandwidth ( $M$ ) suggests an upper bound such that  $L \ll M$ , taken here as one-tenth.
- The number of coefficients of the Laguerre functions in each first-order kernel, before they decay to zero.

The memory of a system can be taken to be the number of points in its first-order kernel until they settle to zero. Both kernels derived by the Lee-Schetzen Technique (LST) and the Laguerre Expansion Technique (LET) can be used for this purpose. If using LET, a few attempts will be required to find a value of  $\alpha$  which will make most of the kernel fit into its assigned number of points.

Finding the number of required coefficients can be easily done by finding the first-order kernel using LET with a large  $L$  and counting their coefficients as they decay to zero. Any reasonable value of  $\alpha$  (say 0.8 to 0.9) will suffice for this first approximation.

### 2.2 Finding and Refining $\alpha$

The  $\alpha$  parameter varies the duration of the Laguerre functions, and thus that of the kernel as a whole. If  $\alpha$  is too high, then the kernel will not fit into its assigned number of points. If  $\alpha$  is too low, then points at the tail end of the kernel will simply remain at zero. In both cases, there is lost information and the quality of the WB model will suffer.

An approximate ideal value of  $\alpha$  can be found by slightly raising or lowering it until the kernel of interest just decays to zero at the end of its assigned number of points. Although the initial estimation of  $\alpha$  yields a working WB model, the fit is improved by comparing the responses of the model with those of the original system, and slightly altering  $\alpha$  until a minimum error is found. In this case, the MODRES program calculates the WB response, and can also report the Mean Square Error (MSE) relative to the FHN response.

#### 2.2.1 Most Significant Kernel

Depending on whether the FHN system being modelled is acting under low or high-power modes of operation, a different kernel becomes dominant in the corresponding WB model. During subthreshold (low-power) behaviour, the FHN system is effectively a linear R-C system, which is modelled by the first-order WB kernel. In suprathreshold (high-power) behaviour, the non-linear aspect of the action potentials is modelled by the second-order WB kernel. Thus, depending on the mode of operation, the value of  $\alpha$  should be chosen to maximize the fit of the corresponding kernel, at the expense of the other, which will usually be overly magnified and thus truncated.

### 3 Results

#### 3.1 FHN System Response

The following two figures show the GWN stimulus and the corresponding response of the FHN system in both subthreshold (low-power) and suprathreshold (high-power) modes:

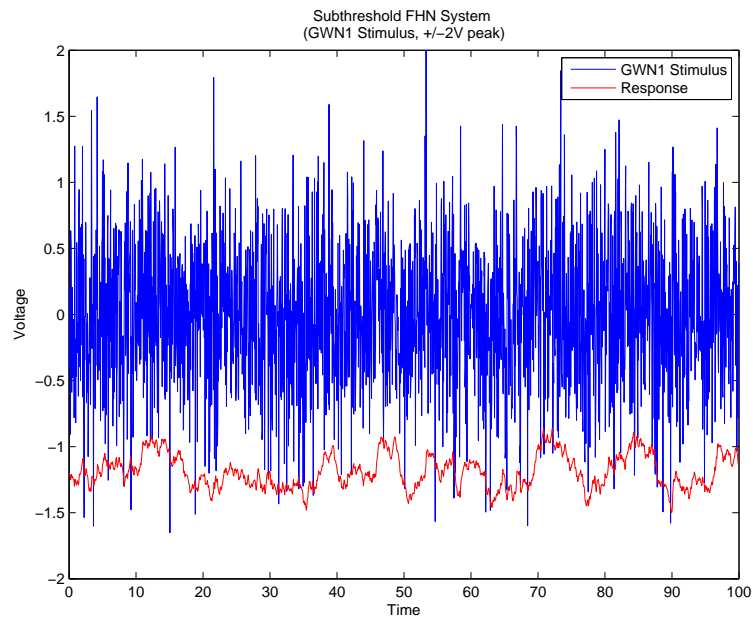


Figure 1: Subthreshold FHN System under GWN1 Stimulus

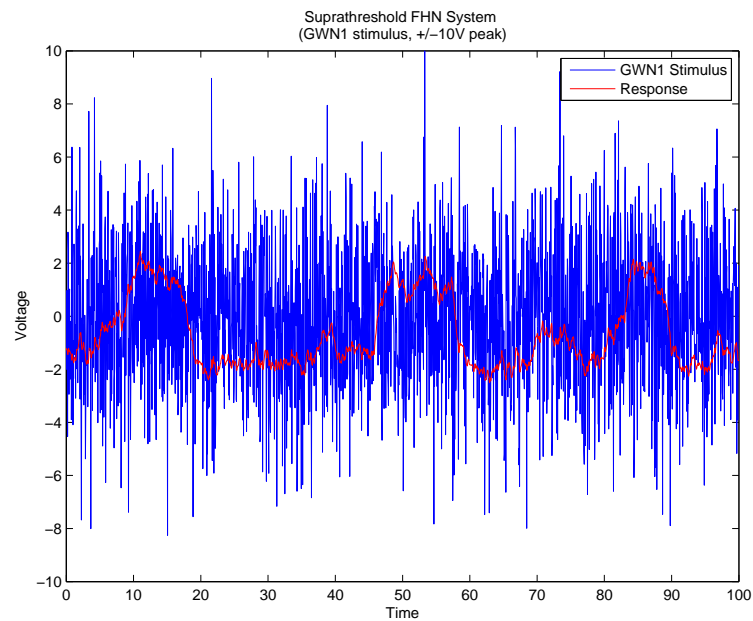


Figure 2: Suprathreshold FHN System under GWN1 Stimulus

## 3.2 Determining $L$

### 3.2.1 Determining $L$ via Memory-Bandwidth Product

The following four figures show the semi-log frequency spectrum of the sub and suprathreshold responses of the FHN system, along with its first-order kernels derived using the Lee-Schetzen Technique provided by the CKER program.

The response bandwidth is not clearly discernible, but most of the drop ( $\sim 100\times$ ) occurs before 1 Hz, and so this value will be assumed as the bandwidth. It is surprisingly low, but consistent across GWN stimuli. It is possible that the FFT MATLAB code was erroneous. However, the calculation of  $L$  by other means supports these results.

The first-order kernels for both modes are similar as expected. Their memory is taken to be the number of points until the first zero-crossing. There are 88 and 130 points for the low and high-power modes. Multiplying these by the bandwidth of one and taking one-tenth of that value as a suitable  $L \ll M$  yields  $L = 9$  for the low-power mode, and  $L = 13$  for the high-power mode.

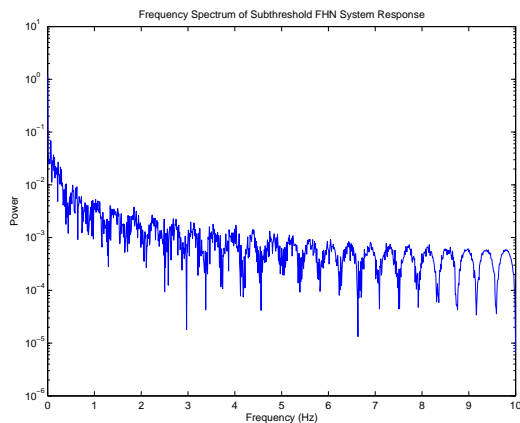


Figure 3: Frequency Spectrum of Subthreshold FHN System Response

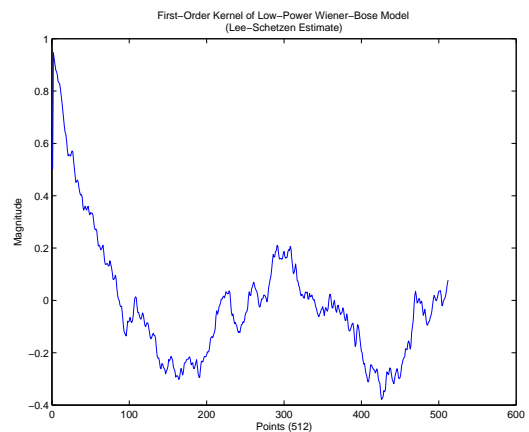


Figure 5: First-Order Lee-Schetzen Kernel of Low-Power Wiener-Bose Model

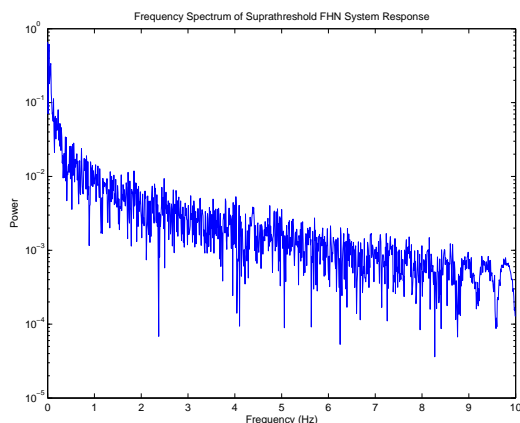


Figure 4: Frequency Spectrum of Suprathreshold FHN System Response

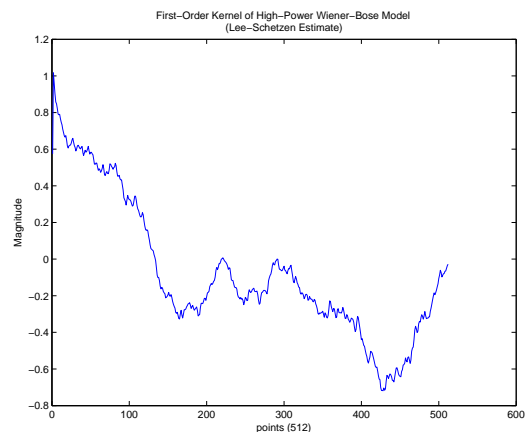


Figure 6: First-Order Lee-Schetzen Kernel of High-Power Wiener-Bose Model

### 3.2.2 Determining $L$ via Laguerre Coefficients

The following two figures show the coefficients of the first-order kernels for both power modes. These are the coefficients of the final, tuned kernels derived using LET. It is clear that  $L = 9$  is sufficient for the low-power mode, but not for the high-power mode. Since  $L = 13$  was suggested by the Memory-Bandwidth product, and it is also the maximum allowed by the CKER program, this value was chosen despite the lack of confirmation that it is sufficient.

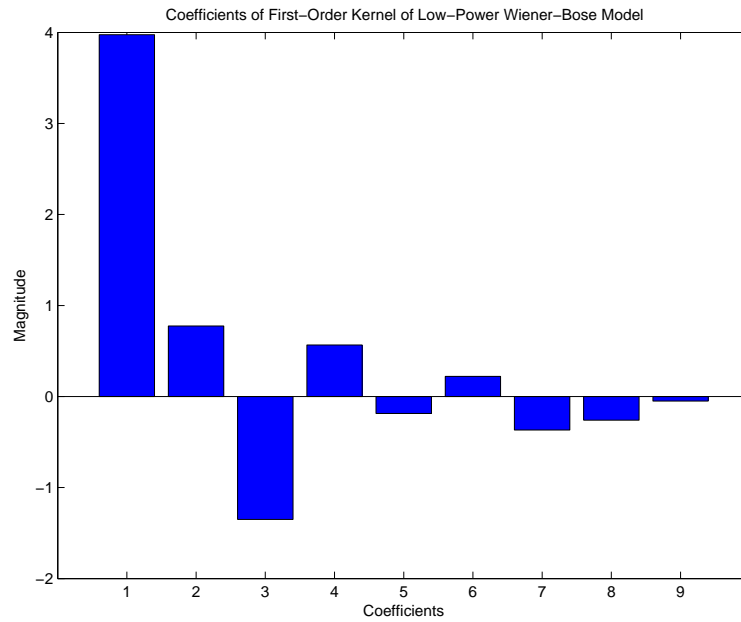


Figure 7: Coefficients of First-Order Kernel of Low-Power Wiener-Bose Model

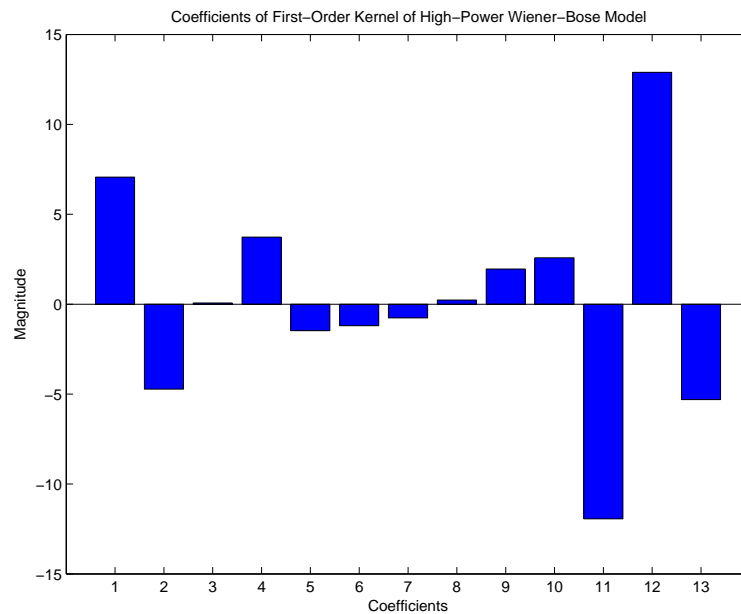


Figure 8: Coefficients of First-Order Kernel of High-Power Wiener-Bose Model

### 3.3 First and Second-Order Kernels

The following four figures show the first and second-order kernels for both the low and high-power modes after fine-tuning  $\alpha$  to minimize the modelling error. The best values found are  $\alpha = 0.95$  and  $\alpha = 0.94$  for low and high-power modes respectively. Additionally, each mode has a zeroth-order kernel which is a simple DC offset on the response: -1.19105 and -0.7403556 for low and high-power modes, respectively.

It is important to note that the  $\alpha$  value was initially adjusted to maximize the fit of the dominant kernel for a given mode. Hence, in the low-power mode, the first-order kernel just fits into its 512 points, while the second-order kernel is truncated, not having enough space to decay to zero. Conversely, the first-order kernel of the high-power mode is a grossly distorted and truncated version of the low-power version since  $\alpha$  is chosen to maximize the fit of the second-order kernel.

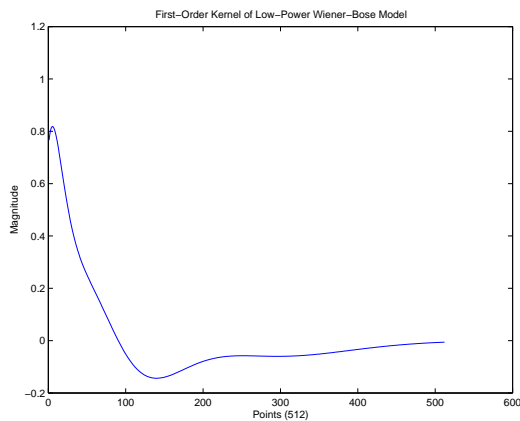


Figure 9: First-Order Kernel of Low-Power Wiener-Bose Model ( $\alpha = 0.95$ )

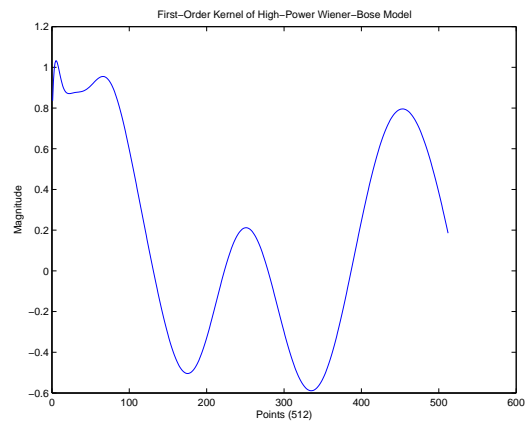


Figure 11: First-Order Kernel of High-Power Wiener-Bose Model ( $\alpha = 0.94$ )

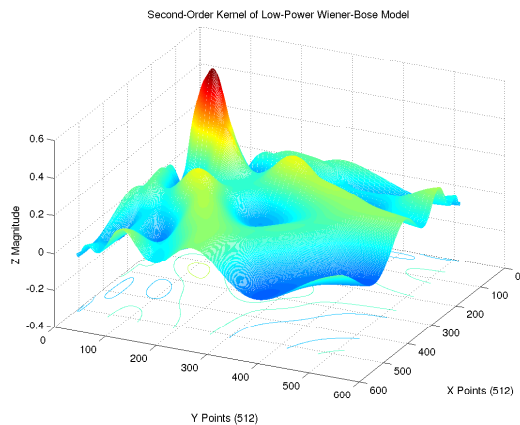


Figure 10: Second-Order Kernel of Low-Power Wiener-Bose Model ( $\alpha = 0.95$ )

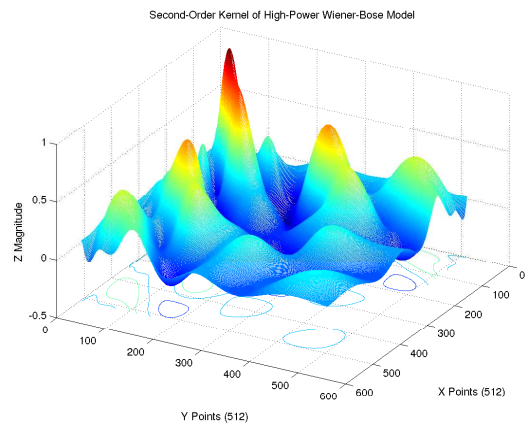


Figure 12: Second-Order Kernel of High-Power Wiener-Bose Model ( $\alpha = 0.94$ )



### 3.4 Wiener-Bose Model under GWN Stimuli

The following six figures compare the resulting WB models to the original FHN system by plotting their responses to three different GWN stimuli generated from different initial seeds, but otherwise identical in spectra, duration, and peak amplitude. In all cases, GWN1 was the stimulus to which the WB model was fitted, while GWN2 and GWN3 were 'new' stimuli aimed at testing the flexibility of the WB models.

#### 3.4.1 Low-Power Mode

The following three figures show the low-power WB model responding to subthreshold GWN stimuli. Even under new GWN stimuli, the model remains reasonably accurate (see Table 1). This is to be expected since in the absence of action potentials, the FHN system is merely a linear R-C system.

MSE of Low-Power WB Model	
Stimulus	Mean Square Error
GWN1	$2.469 \times 10^{-4}$
GWN2	$1.203 \times 10^{-3}$
GWN3	$3.604 \times 10^{-3}$

Table 1: Mean Square Error of Low-Power WB Model Response Relative to FHN System Response

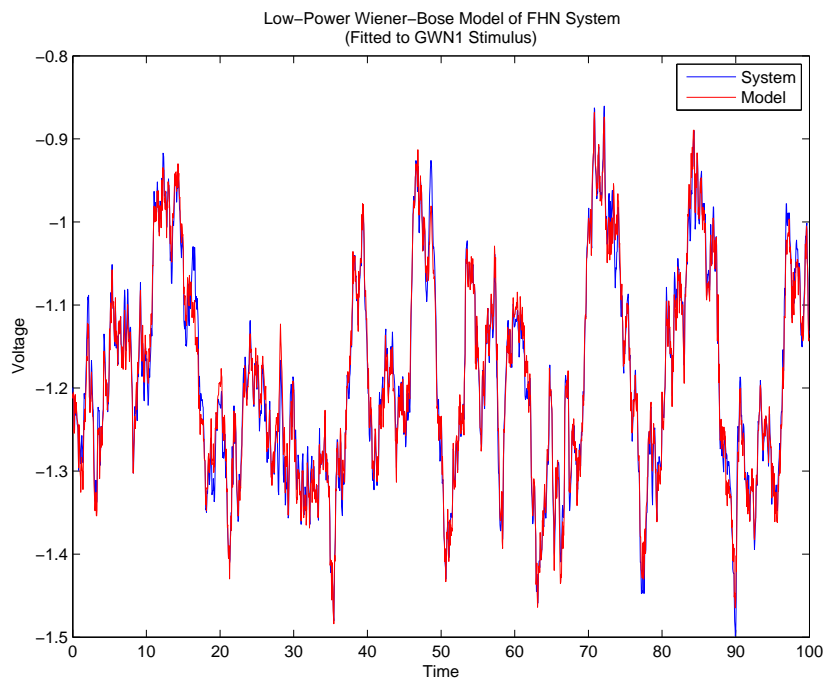


Figure 13: Comparison of Low-Power Wiener-Bose Model to FHN System (GWN1)

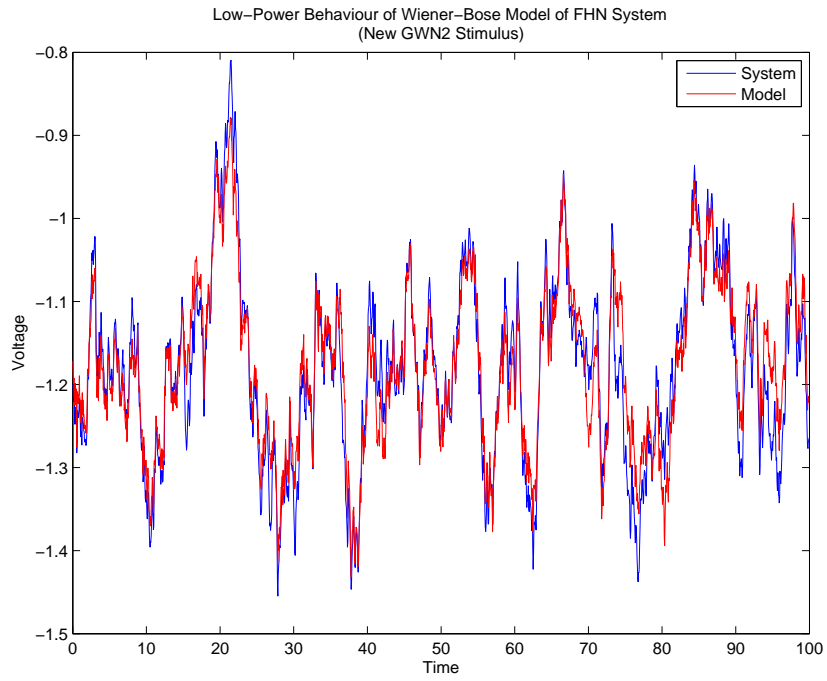


Figure 14: Comparison of Low-Power Wiener-Bose Model to Subthreshold FHN System(GWN2)

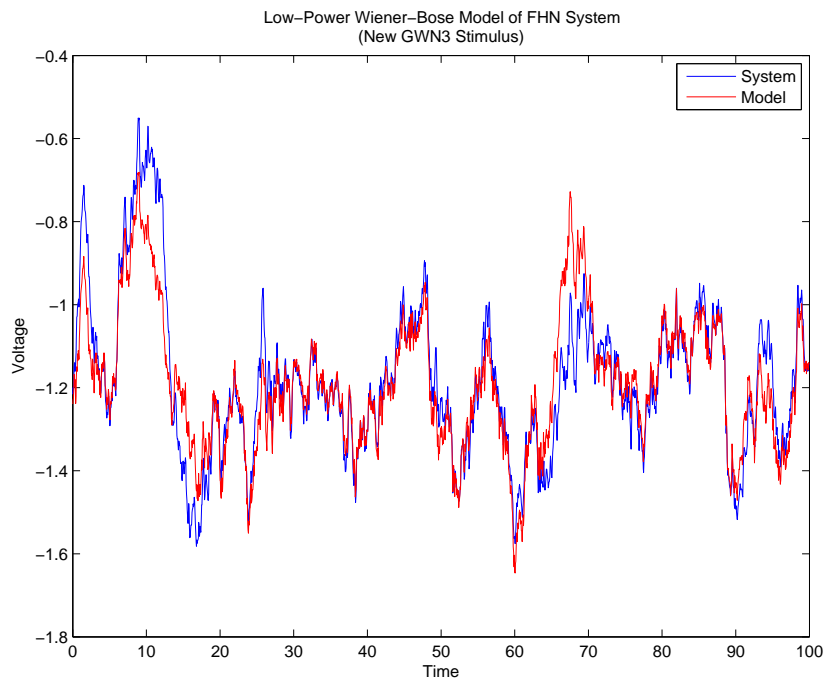


Figure 15: Comparison of Low-Power Wiener-Bose Model to Subthreshold FHN System (GWN3)

### 3.4.2 High-Power Mode

The following table and three figures show the high-power WB model responding to suprathreshold GWN stimuli. The non-linear behaviour is more difficult to model, and fails almost completely to model unknown stimuli. Actually, if one looks closely at the WB model response, we can see short periods (0 to 20s for GWN2, and 35 to 45s for GWN3) where its response closely matches that of the FHN system before wildly veering off.

MSE of High-Power WB Model	
Stimulus	Mean Square Error
GWN1	$2.119 \times 10^{-2}$
GWN2	3.720
GWN3	18.21

Table 2: Mean Square Error of High-Power WB Model Response Relative to FHN System Response

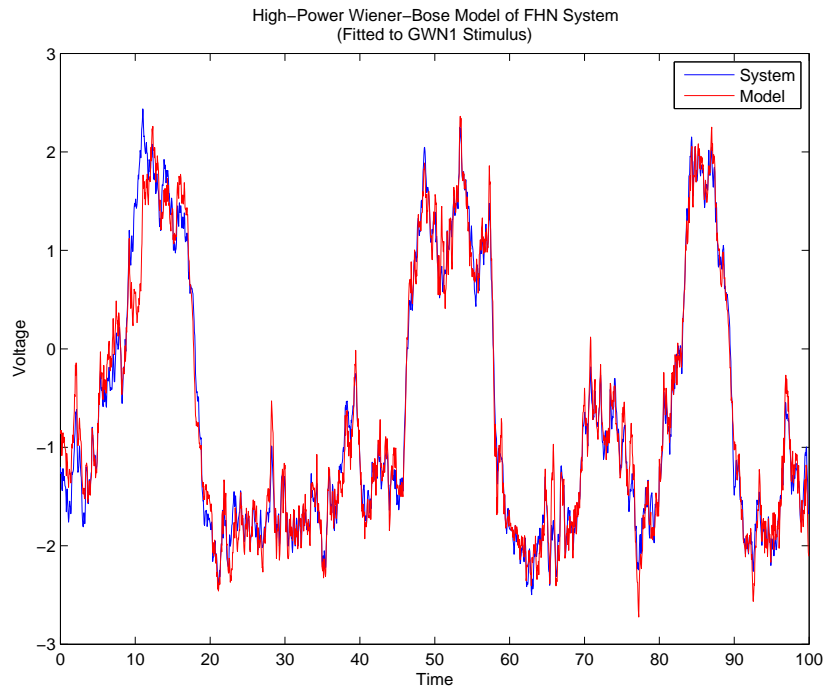


Figure 16: Comparison of High-Power Wiener-Bose Model to Suprathreshold FHN System (GWN1)

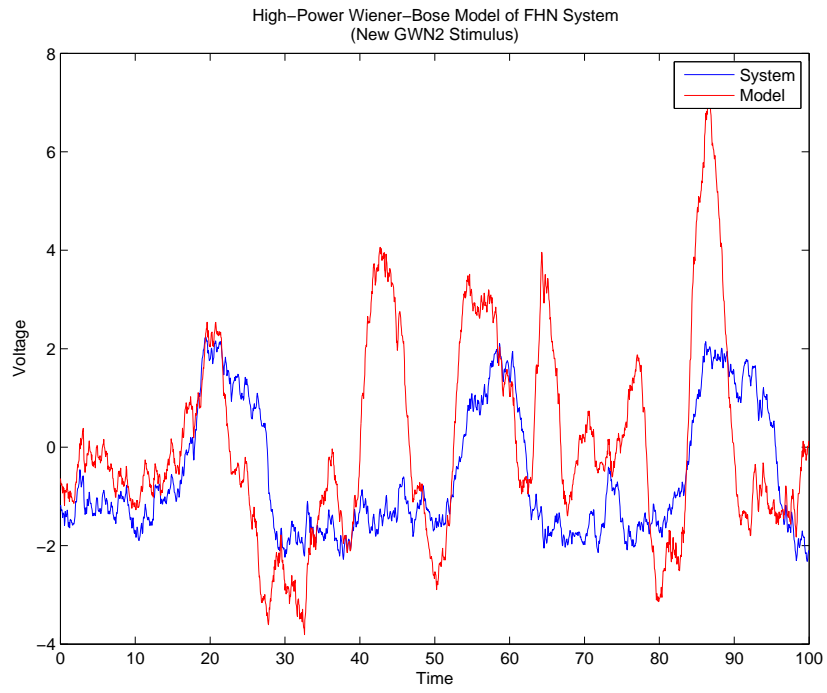


Figure 17: Comparison of High-Power Wiener-Bose Model to Suprathreshold FHN System (GWN2)

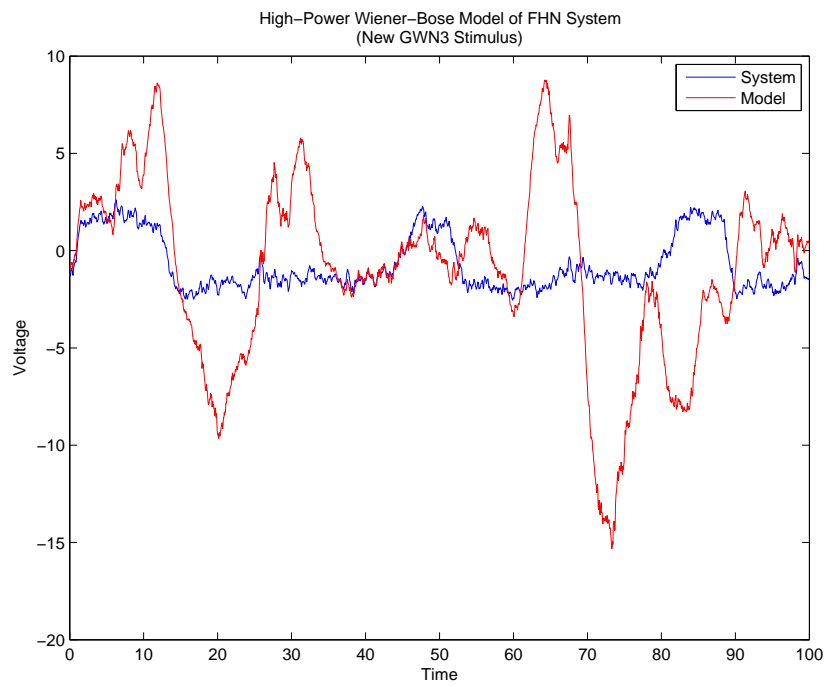


Figure 18: Comparison of High-Power Wiener-Bose Model to Suprathreshold FHN System (GWN3)

### 3.5 Wiener-Bose Model under Other Stimuli

The WB model is only an input-output map with a finite memory, and does not have internal feedback as in the FHN system where  $V$  and  $W$  are functions of each other. A good fit to a given input can be obtained since the coefficients for each Laguerre function are adjusted via a Least-Squares fit, but this fit is rigid and will not suit other inputs which take the model into other sequences of internal states as defined by the contents of its finite memory. This qualitatively explains why even for GWN inputs, which should not favour one set of internal states over others, the response of the WB model can vary wildly from that of the FHN system, while still occasionally being correct.

#### 3.5.1 Low-Power Mode under Constant Stimulus

The following five figures compare the response of the low-power WB model and the original FHN system under different constant stimuli. The behaviour under a zero stimulus is obviously correct as only the zeroth-order kernel, which mimics the resting state of the FHN system, has any effect. However, for all other constant stimuli, the model is completely wrong. Mostly this is due to the original system having action potentials, which are not modelled by the low-power model. A constant input seems to saturate the convolutions. Note that the saturation occurs after exactly 512 samples (Each sample is at a time-step of 0.05, hence  $512 \times 0.05 = 25.6$ .), and obviously mirrors the structure of the first-order kernel.

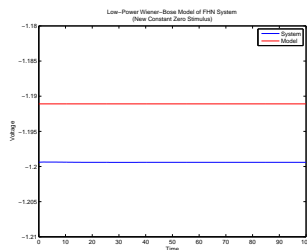


Figure 19: Low-Power Wiener-Bose Model of FHN System (Constant Zero Stimulus)

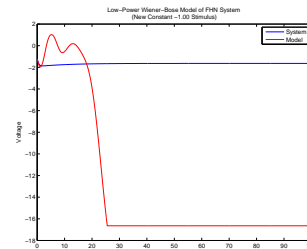


Figure 22: Low-Power Wiener-Bose Model of FHN System (Constant -1 Stimulus)

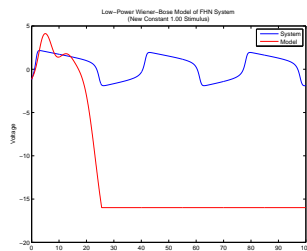


Figure 20: Low-Power Wiener-Bose Model of FHN System (Constant 1 Stimulus)

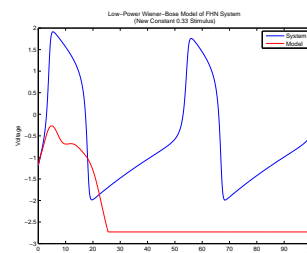


Figure 23: Low-Power Wiener-Bose Model of FHN System (Constant 0.33 Stimulus)

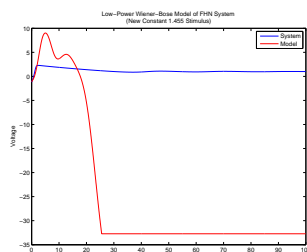


Figure 21: Low-Power Wiener-Bose Model of FHN System (Constant 1.455 Stimulus)

### 3.5.2 Low-Power Mode under Periodic Stimulus

Under periodic inputs of various frequencies and amplitudes, the low-power WB model also fares poorly, again due to non-linearities in the FHN system due to evoked action potentials. The one exception is for a  $0.33\cos(t)$  stimulus (Figure 27), which does not trigger action potentials in the FHN system. Correspondingly, the low-power WB model outputs a reasonable attempt at matching the response since this periodic input has an average of zero over time and thus does not saturate the model's memory.

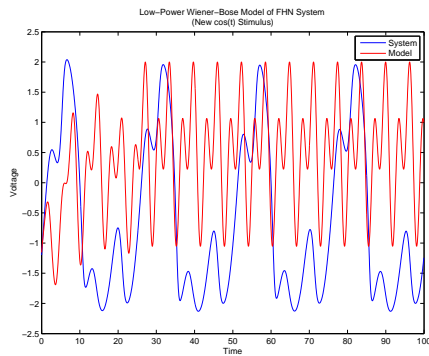


Figure 24: Low-Power Wiener-Bose Model of FHN System ( $\cos(t)$  Stimulus)

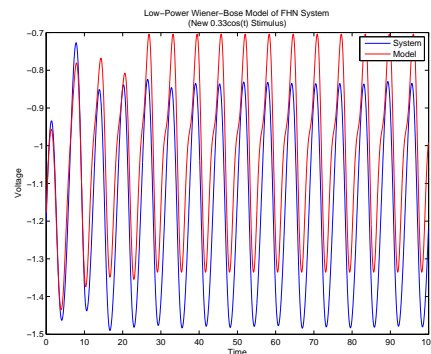


Figure 27: Low-Power Wiener-Bose Model of FHN System ( $0.33\cos(t)$  Stimulus)

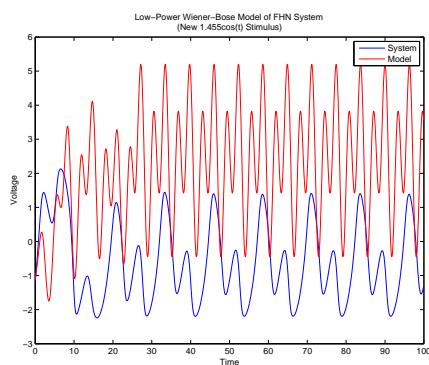


Figure 25: Low-Power Wiener-Bose Model of FHN System ( $1.455\cos(t)$  Stimulus)

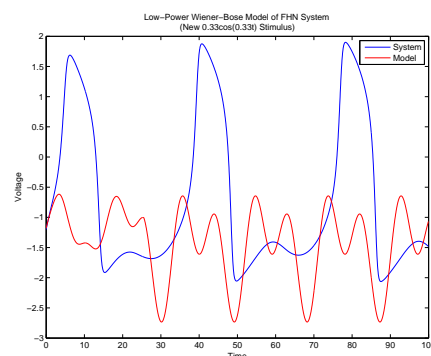


Figure 28: Low-Power Wiener-Bose Model of FHN System ( $0.33\cos(0.33t)$  Stimulus)

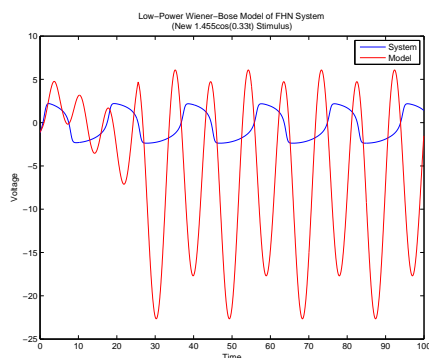


Figure 26: Low-Power Wiener-Bose Model of FHN System ( $1.455\cos(0.33t)$  Stimulus)

### 3.5.3 High-Power Mode under Constant Stimulus

The behaviour of the high-power WB model under constant stimulus is identical to that of the low-power model, again due to the saturation of the model's memory. (Note that the caption on Figure 30 is incorrect: the stimulus is one, not zero.)

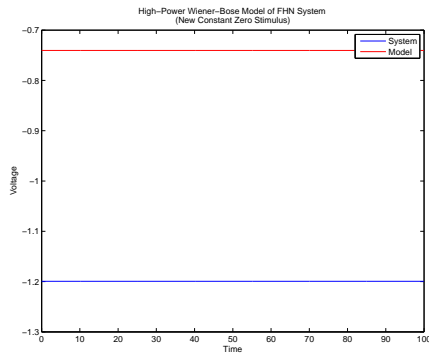


Figure 29: High-Power Wiener-Bose Model of FHN System (Constant 0 Stimulus)

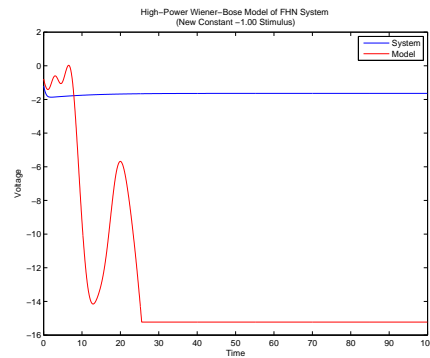


Figure 32: High-Power Wiener-Bose Model of FHN System (Constant -1 Stimulus)

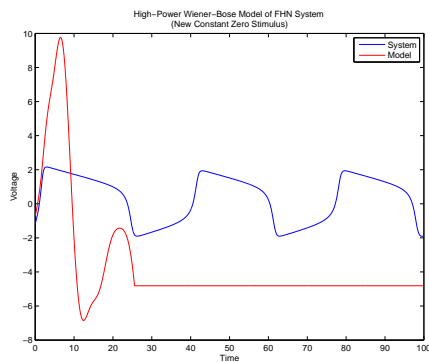


Figure 30: High-Power Wiener-Bose Model of FHN System (Constant 1 Stimulus)

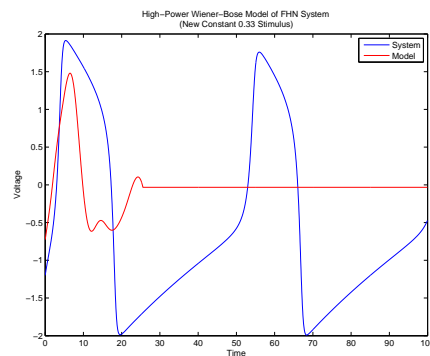


Figure 33: High-Power Wiener-Bose Model of FHN System (Constant 0.33 Stimulus)

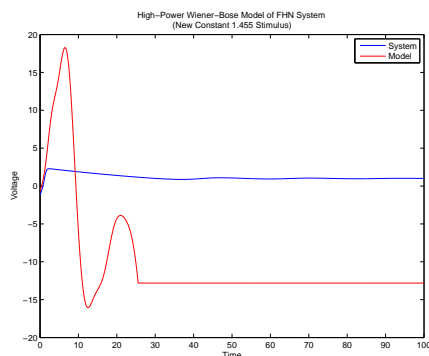


Figure 31: High-Power Wiener-Bose Model of FHN System (Constant 1.455 Stimulus)

### 3.5.4 High-Power Mode under Periodic Stimulus

Under periodic input, the high-power WB model fares better than the low-power version, but is still mostly a very poor match. The output magnitude are almost always too high, despite being similar to the output of the FHN system. This suggests that there is interaction between multiple cycles inside the model's memory, yielding a periodic pattern of reinforcement and cancellation.

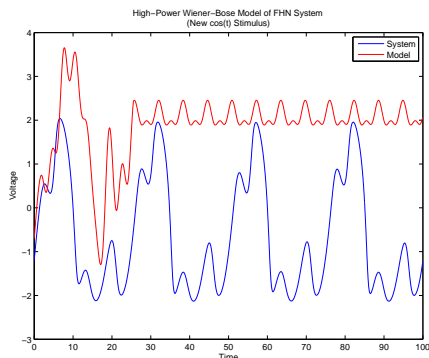


Figure 34: High-Power Wiener-Bose Model of FHN System ( $\cos(t)$  Stimulus)

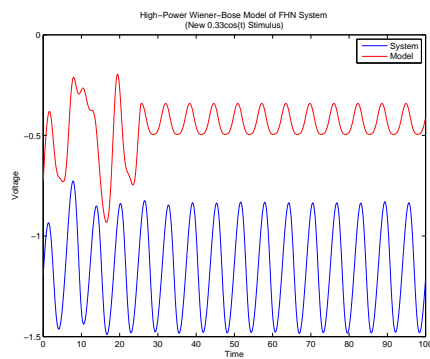


Figure 37: High-Power Wiener-Bose Model of FHN System ( $0.33\cos(t)$  Stimulus)

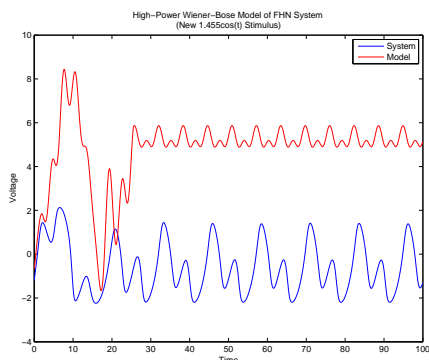


Figure 35: High-Power Wiener-Bose Model of FHN System ( $1.455\cos(t)$  Stimulus)

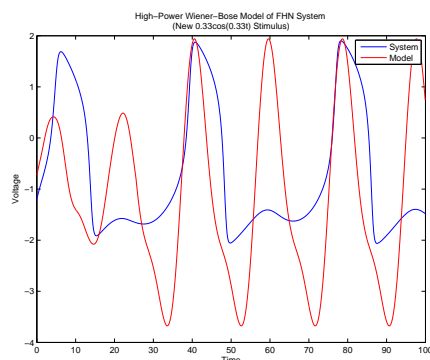


Figure 38: High-Power Wiener-Bose Model of FHN System ( $0.33\cos(0.33t)$  Stimulus)

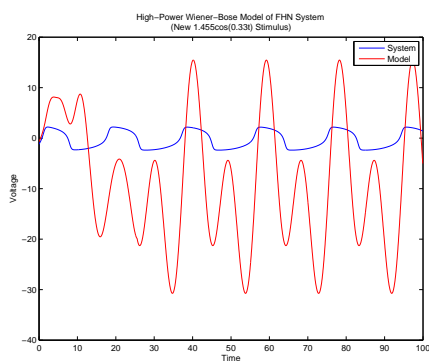


Figure 36: High-Power Wiener-Bose Model of FHN System ( $1.455\cos(0.33t)$  Stimulus)